Results in Engineering 6 (2020) 100113

Contents lists available at ScienceDirect

Results in Engineering

journal homepage: www.editorialmanager.com/rineng/Default.aspx

Simultaneous and continuous biosorption of Cr and Cu (II) ions from industrial tannery effluent using almond shell in a fixed bed column

M.D. Yahya [a], H. Abubakar [a], K.S. Obayomi [b,*], Y.A. Iyaka [c], B. Suleiman [d]

[a] Department of Chemical Engineering, Federal University of Technology Minna, Niger State, Nigeria
[b] Department of Chemical Engineering, Landmark University Omu-Aran, Kwara State, Nigeria
[c] Department of Chemistry, Federal University of Technology Minna, Niger State, Nigeria
[d] Department of Chemical Engineering, Usman Dan Fodio University, Sokoto State, Nigeria

ARTICLE INFO

Keywords:
Almond shell
Tannery effluent
Heavy metals
Column adsorption

ABSTRACT

The study on performance of almond shell in the simultaneous removal of Cr ions and Cu (II) from tannery effluent was investigated in a laboratory scaled fixed bed column. The characterization of the almond shell was examined using SEM (scanning electron microscope) and FTIR (Fourier transform infrared spectroscopy). FTIR analysis of almond shell revealed the existence of hydroxyl, carbonyl and aliphatic functional groups responsible for the adsorption of the metal ions. The breakthrough curve basically was used to study the efficiency of the packed bed adsorption system with the almond shell. It was observed that the breakthrough is a function of flow rate, initial metal concentrations and the packed bed height. The column adsorption effectiveness increases with the rise in the influent concentration, bed depth and reduces with the rise in the flow rate. The column parameters analysed indicated the efficiency of the column at flow rate of 3.0 ml/min, bed height of 7.0 cm and concentrations of 67.5 mg/L and 7.0 mg/L for Cr ions and Cu (II) ions respectively. The proportional removal of Cu (II) and Cr ions at optimal values were 70.0 and 65.9% with adsorption capacities of 2.39 and 21.92 mg/g respectively. Column adsorption kinetics was sufficiently defined with Thomas and Yoon and Nelson models. The model parameters, such as mass transfer coefficient and kinetic parameters were determined. Comparison between experimental breakthrough curves to the breakthrough profiles determined using Thomas and Yoon-Nelson models gives prominent correlation coefficients (R^2) indicating satisfactory fit for both metals.

1. Introduction

Wastewater comprising of heavy metals are unceasingly discharged from thousands of large-scale and small-scale industries, including leather tanning, battery manufacturing, chemical manufacturing, metallurgy, mining sites drainage, and electroplating industries, particularly in developing countries. These are discharged into the natural water sources either directly or indirectly, mostly without appropriate treatment, posing a significant hazard to the surroundings [1,2]. Heavy metals are particularly hazardous pollutants that can gather in the tissues of living organisms triggering various disorders and illnesses [3]. Owing to their toxicity even at lessened concentrations, the influence of heavy metals in the wastewater of several industrial procedures has caused more environmental concerns [3,4]. Some of the core toxic metal ions which are particularly dangerous to humans and aquatic habitat are arsenic (As), copper (Cu), iron (Fe), zinc (Zn), cobalt (Co), selenium (Se), chromium (Cr), nickel (Ni), mercury (Hg), lead (Pb), and cadmium (Cd) [2]. Given that all heavy metals are non-biodegradable; to achieve environmental quality standards they must be eliminated or decreased to threshold point before discharge into water bodies. The tanning industry has been identified as one of the largest polluters all over the world [5]. It is one of the major consumers of water which is usually discharged as wastewater containing great amount of heavy metals particularly chromium and copper [6]. The enormous pollution load in addition to the toxic characteristics of wastewater makes the tanneries a probable threat to its neighbouring communities as it constitutes a serious health hazard. Though, tanneries provide revenue and job opportunities, their effluent pollution challenges are the major issues of concern.

The conventional wastewater treatment such as chemical coagulation [7], membrane separation [8], solvent extraction [9], ion-exchange [10], chemical precipitation [11] and more recently electrochemical degradation [12] are applied in treating water and remove heavy metals.

* Corresponding author.
E-mail addresses: muibat.yahya@futminna.edu.ng (M.D. Yahya), obayomi.kehinde@lmu.edu.ng (K.S. Obayomi).

https://doi.org/10.1016/j.rineng.2020.100113
Received 3 December 2019; Received in revised form 6 March 2020; Accepted 9 March 2020

However, a number of these necessitate the application of costly chemicals and complex technology and thus they are often not low-priced when considering removing lower concentration of heavy metals [13, 14]. Furthermore, heavy metals removal through precipitation and coagulation techniques results into the formation of sludge requiring additional treatment for safe disposal [15]. From the afore mentioned limitations of most of the conventional technologies, adsorption approach is the simplest prominent method to use considering its great competence, effortlessness in handling, cost effectiveness, adsorbent availability and insensitivity to toxic substance [16–18].

The most used commercial adsorbent for the removal of heavy metal wastewater is the activated carbon. Nevertheless, it is still a costly and sophisticated material [19]. This has gripped the curiosity of researchers to intensify the venture for inexpensive adsorbents with metal-binding dimensions [16]. Several researches have been conducted in discovering cost-effective and available agricultural deposit materials including hazelnut husk [20], palm shell [21], groundnut shell [22], rice husk [23], palm date pits [16], mango seed [24], coconut shell [25], wheat bran [26], banana peel [27], shea butter husk [28], almond leaves [29] and almond shell [30] as adsorbents to remove heavy metals from aqueous solutions. Furthermore, a more comprehensive review on different kind of materials, both agricultural wastes, non-agricultural wastes and other materials type used as adsorbents for heavy metals removal have been reported in literature as cited by Ref. [31–33] to mention a few.

The application of almond shell as an adsorbent has been carefully examined in activated system. Few metals such as Fe, Zn, Co, and Ni have been investigated in batch method adsorption and have indicated encouraging outcomes. However, most of the studies have concentrated on batch studies for the removal of a single contaminant which cannot solve a community problem and fewer researches are available for continuous process [34]. Column experiments are essential to deliver data which can be applied for industrial purposes. However, to the best knowledge of the author, information on the application of almond shell for continuous and the simultaneous removal of Cr ions and Cu (II) ions from tannery wastewater in column mode adsorption technique are limited if not non-existence in literature. Therefore, this research is aimed at using raw almond shells as an adsorbent for the simultaneous removal of Cu (II) and Cr ions in a real tannery effluent by means of a column method of adsorption process.

2. Materials and methods

2.1. Collection and preparation of adsorbent

The almond fruit shells were obtained from a farmyard in Kabba area of Kogi State, Nigeria. The almond shells were sorted out, cut to lesser fragments, cleaned severally with water from the tap and distilled water to eliminate exterior filth. The wetted almond shells were spread under atmospheric air to remove excess water from the exterior and then dried in the oven for 24 h at 100 ^{O}C. The dried almond shells were crushed and sifted to particle size of 200–350 μm. This was preserved in tightly sealed container for further use.

2.2. Characterization of adsorbent

The almond shells were characterized using various techniques. FTIR spectroscopy was applied to indicate the functional sets available on the almond shells before and after adsorption process. The samples were observed by means of spectrophotometer at the scale of 650–4000 cm^{-1}. Potassium bromide (KBr) was applied as frame works in the work and the spectra were recorded through a FT-IR spectrophotometer (8400 S Agilent Technologies). The exterior morphology of the almond shell before and the adsorption procedure was also, studied using a scanning electron microscopy (DSM 9872 Gemni SEM).

2.3. Collection of tannery effluent

The tannery effluent was collected from Fata Tanning Industry in Challawa Industrial Estate Kano State, Nigeria. The effluent was preserved in elastic vessels and the concentrations of the heavy metals in the effluent sample were analysed using Atomic Absorption Spectrometer (ICE3000AA Thermo scientific).

2.4. Column adsorption procedure

Column adsorption experiment was carried out with the aid of a glass column of 3 cm internal diameter and 30 cm length. The column was packed with almond shells of particle size range of 0.25–0.35 mm between dual supporting layers of glass beads and glass wool to prevent the falling out of the adsorbent from the outlet as revealed in Fig. 1. The column efficiency study was to assess the impacts of several operating parameters such as the initial metal concentrations, bed heights, and flow rates. The wastewater was passed through the bed in the down-flow mode at varying flow rates in the range of 3–9 ml/min, metals concentrations range of 50-70 mg/L and 3.5–7.0 mg/L, bed heights of 3–7 cm, for Cr and Cu (II) ions, correspondingly. The wastewater was allowed into the column continuously from its storage tank by gravitational flow. The process consists of reservoir 1 and 2 connected in series to maintain continual flow rate into reservoir 2 and afterwards, to the column, by the use of control valve to maintain a continuous solution level in the tank that ensured zero fluctuation of solution flow to the column. The effluent samples were taken at definite periods and analysed for residual Cr ions and Cu (II) concentrations by means of Atomic Absorption Spectrometer (AAS). The sample collection was stopped when the influent concentrations almost equals the outlet concentration.

2.5. Column performance evaluation

The portion underneath the breakthrough curve is the cumulative mass of heavy metals adsorbed q_{total} (mg) for a given feed concentration and flow rate according to Eq. (1) reported by Refs. [35]:

$$q_{total} = \frac{Q}{1000}\int_{t=0}^{t=t_{total}} C_R\,dt \quad [1]$$

where C_R is the concentration of metal removed in mg/L, Q is the volumetric flow rate in ml/min and t_{total} is the total flow time in minutes.

The total metal ions dispatched to the pillars in mg were established using Eq. (2).

$$m_{total} = \frac{C_o Q t_{total}}{1000} \quad [2]$$

The percentage removal of metal ions is the ratio of mass of metal adsorbed (q_{total}) to the total mass of metal ions dispatched to the column (m_{total}) given by Eq. (3) [35]:

$$\%R = \frac{q_{total}}{m_{total}} \times 100 \quad [3]$$

The total capacity treated, V_{eff} (ml), is established from Eq. (4) [36]:

$$V_{eff} = Qt_{total} \quad [4]$$

The equilibrium uptake (qe), that is, the amount of metal adsorbed (mg) per unit dry weight of adsorbent (mg/g) in the column, is established using Eq. (5) [37]:

$$q_e = \frac{q_{total}}{m} \quad [5]$$

where m is the mass of adsorbent in the column (g).

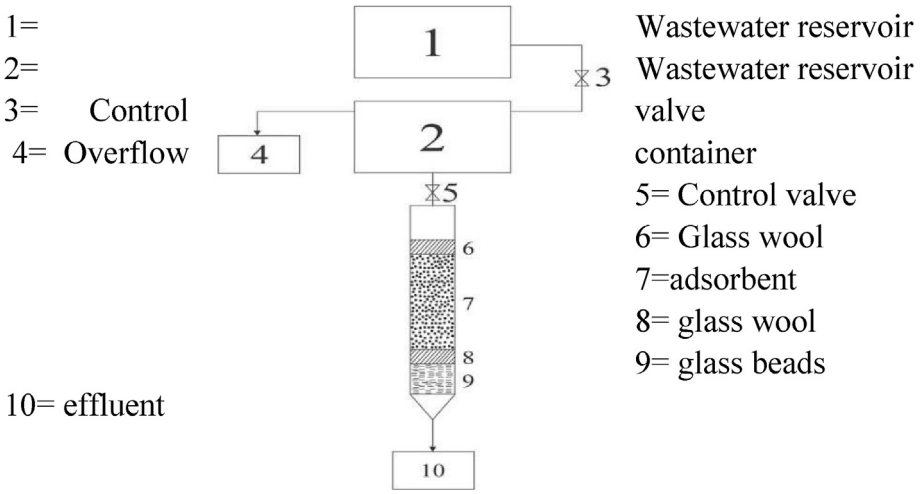

Fig. 1. Schematic diagram of fixed bed adsorption column experiment.

2.6. Modelling of column dynamic behaviour

The effective design of a column adsorption process rests on appropriate prediction of the concentration-time profile or breakthrough curve for effluent concentrations. Several empirical models have been established for the application in the design of constant fixed bed biosorption columns. In this analysis, Thomas and Yoon–Nelson models were used to predict the performance of the breakthrough curve and reported to adequately describe the fixed bed column performance analysis [19,38].

2.6.1. Thomas model

Effective design of a column adsorption process necessitates the prediction of the concentration-time profile or breakthrough curve for the effluent. The maximum adsorption capacity of a biosorbent is likewise required in the construct. Conventionally, the Thomas model is applied to achieve this aim. The model has two forms, Eq. (6) and its linearized frame in Eq. (7) respectively [39].

$$\frac{C_e}{C_0} = \frac{1}{\left(1 + exp\left[\frac{K_T(q_0 m - C_0 V)}{\theta}\right]\right)} \quad [6]$$

where, K_T is the Thomas rate constant (l/(min mg)) and θ is the volumetric flow rate (l/min). The linearized form of the Thomas model is given as Eq. (7):

$$In\left(\frac{C_o}{C_e} - 1\right) = \frac{K_T q_{0m}}{\theta} - K_T C_0 t \quad [7]$$

The kinetic coefficient K_T and the adsorption volume of the bed q_o can be established from a plot of $\ln(C_0/C_e\text{-}1)$ against t.

2.6.2. Yoon and Nelson model

The model is based on the postulation that the rate of reduction in the probability of adsorption for every adsorbate molecule is directly proportional to the probability of adsorbate adsorption and the probability of adsorbate breakthrough on the adsorbent. The Yoon and Nelson model does not only have a reduced level of complexities, but also involves less exhaustive data relating to the features of adsorbate, the physical features of the adsorption bed, and the form of adsorbent. The Yoon and Nelson equation is given in Eq. (8) and its linearized form by Eq. (9) [40]:

$$\frac{C_e}{C_0} = \frac{1}{1 + exp[K_T(\tau - t)]} \quad [8]$$

where k is the rate constant (min^{-1}), τ the time needed for 50% adsorbate breakthrough (min), while t is the breakthrough (sampling) time (min). The linearized form of the Yoon and Nelson model is indicated in Equation (9):

$$t = \tau + \frac{1}{k}\ln\left(\frac{C_0}{C_e - C_0}\right) \quad [9]$$

The evaluation of hypothetical breakthrough curves for a single-constituent system necessitates the determination of the constant, k and τ for the adsorbate of interest. These rates could be determined from the experimental data. The derivation for Eq. (9) was based on the fact 50% breakthrough of the adsorption process would happen at τ and that the bed should be totally saturated at 2τ. Owing to the proportionate characteristics of breakthrough curve, there is a partial quantity of metal adsorbed by the biosorbent of the cumulative metal ions going into the adsorption column within the 2τ duration. The adsorption volume could be established by means of Eq. (10) [41]:

$$q_{total} = \frac{1}{2}C_0\theta(2\tau) = C_0\theta\tau \quad [10]$$

where C_0 is the inlet concentration, θ liquid flow rate and τ is the time to achieve 50% adsorbate breakthrough.

3. Results and discussion

3.1. Characterization of adsorbent

3.1.1. Fourier transform infrared (FTIR) analysis of the adsorbent

The FTIR spectra of almond shell prior to and after adsorption are demonstrated in Figs. 2 and 3 correspondingly. The FTIR spectra indicated the presence of numerous functional groups detected on the exterior of the adsorbent. The different functional groups available on the adsorbent include O–H stretching, C–H stretching, O–CH_3 stretching and C═O stretching. FT-IR spectrum of the raw almond shell sample illustrates a broad and peak at 3328.5 cm^{-1} attributed to the stretching of O–H set because of intra and inter-molecular hydrogen bonding of polymeric compounds such as alcohols or phenols. The peak detected at 2918.5 cm^{-1} was associated with the stretching vibrations of C–H bond of aliphatic group. The peak at 1982.5 cm^{-1}paralleled the C═O stretching could be ascribed to the existence of carbonyl groups. FTIR spectrum of the loaded almond shell after Cr ions and Cu (II) adsorption indicated that the peaks at 3328.5, 1982.9, 1222.6 cm^{-1} (prior to adsorption) had vaguely fluctuated subsequent to binding with the metals. This occurred because of the pores acting as anchoring sites for the Cr and Cu (II) ions [18]. The fluctuation of the wave quantity is subject to the concentration of metals existing in the given model as

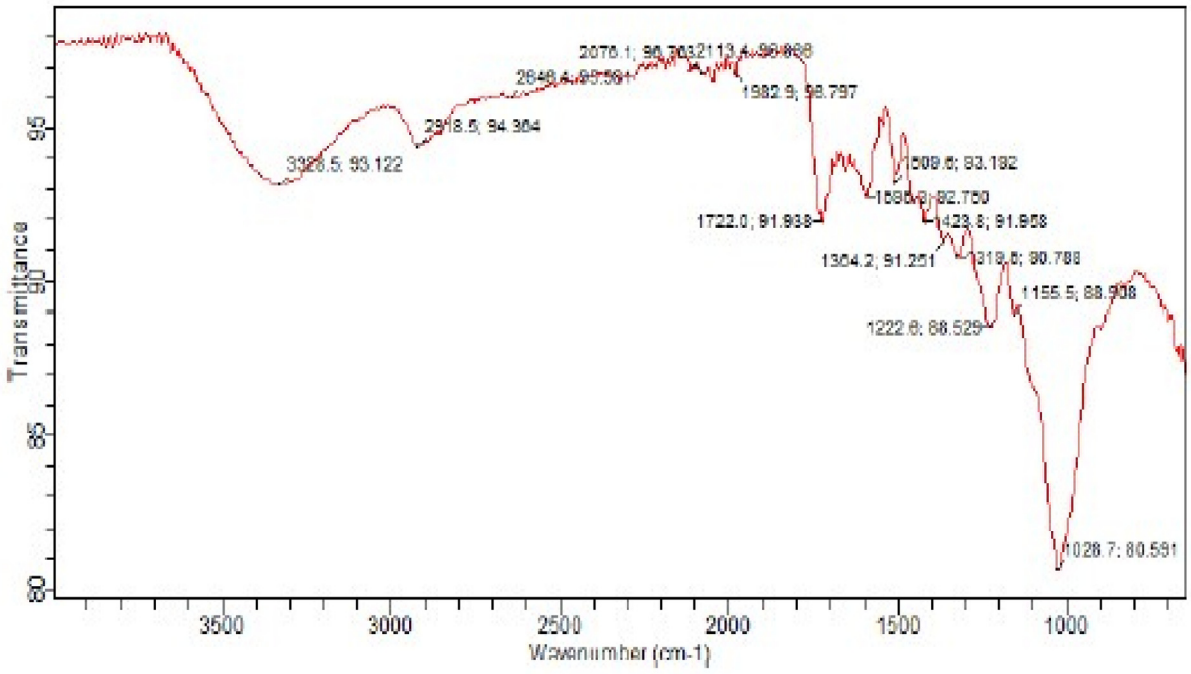

Fig. 2. FTIR spectra of Almond shell prior to adsorption.

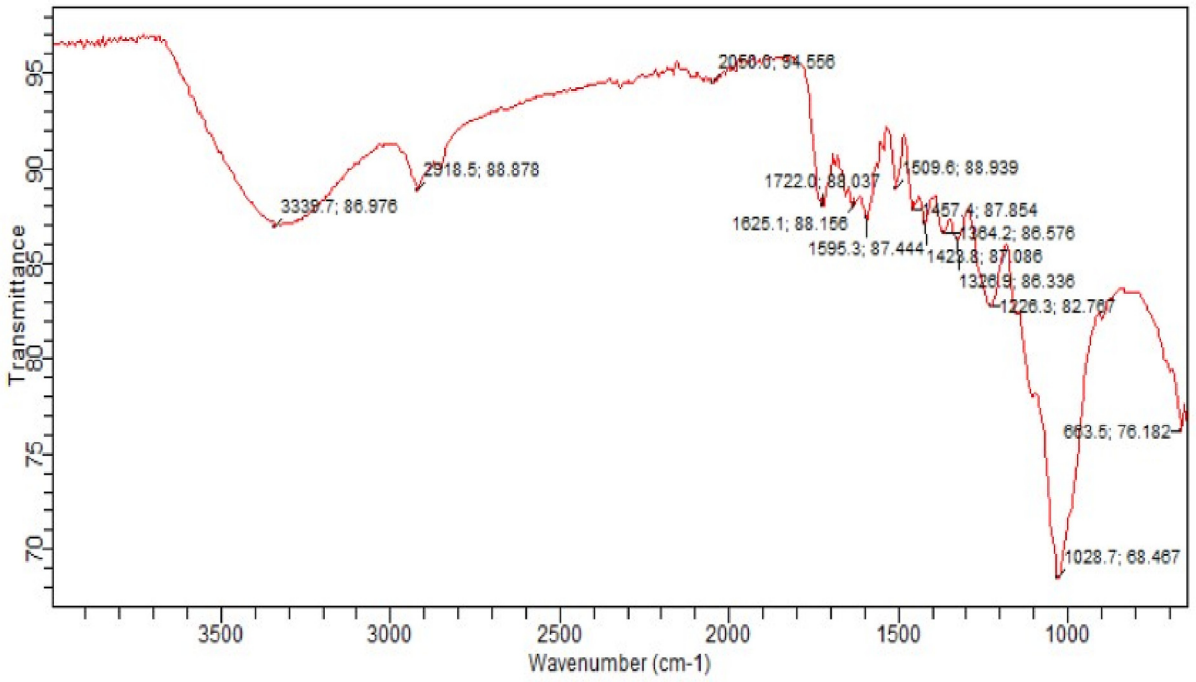

Fig. 3. FTIR spectra of Almond shell after adsorption.

reported in literature [42].

3.1.2. Scanning electron microscopy studies

The adsorbent surface morphology was examined through a scanning electron microscopy (SEM) in Figs. 4 and 5. The SEM representations of almond shell prior to adsorption at magnifications of500X and 1000X in Fig. 4 indicate that the exterior of the adsorbent material was porous. Fig. 5 shows the Cr and Cu (II) ions loaded sites at magnification of 500X and 1000X. Similar study by Refs. [34] was also recorded at lower magnification of 600X. It is evident from the SEM images that the exterior of the sample was coarse and contained porous structure of different shapes and sizes. The interior cavities in the porous structure offer new sites for adsorption of the metal ions.

3.2. Tannery effluent composition

The initial pH of the wastewater sample was analysed to be 3.7. This implies that the wastewater is highly acidic. Using the atomic-absorption

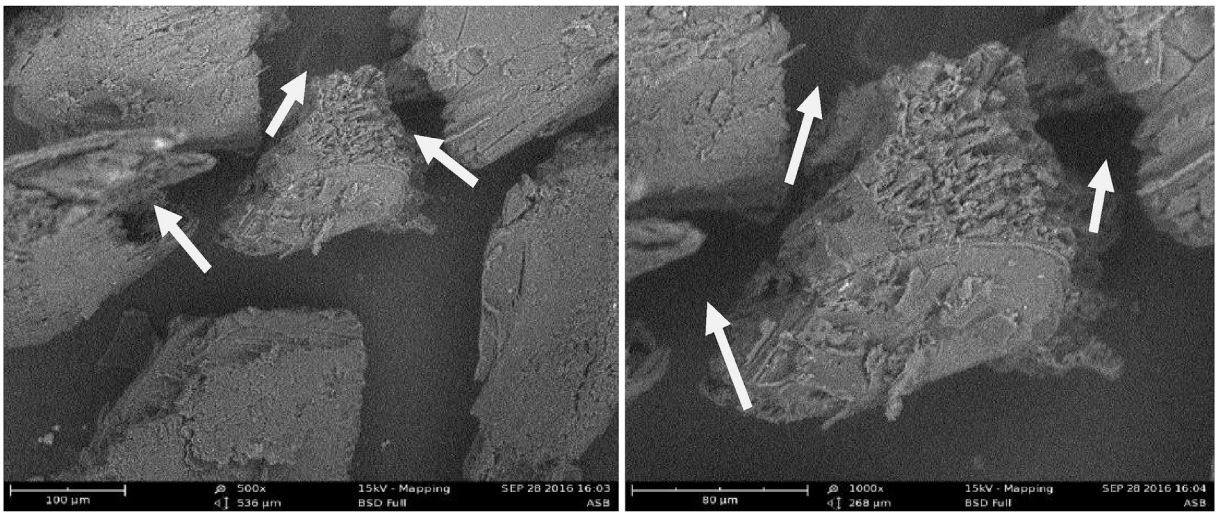

Fig. 4. SEM representations of raw almond shell at different magnification (A) 500, (B) 1000.

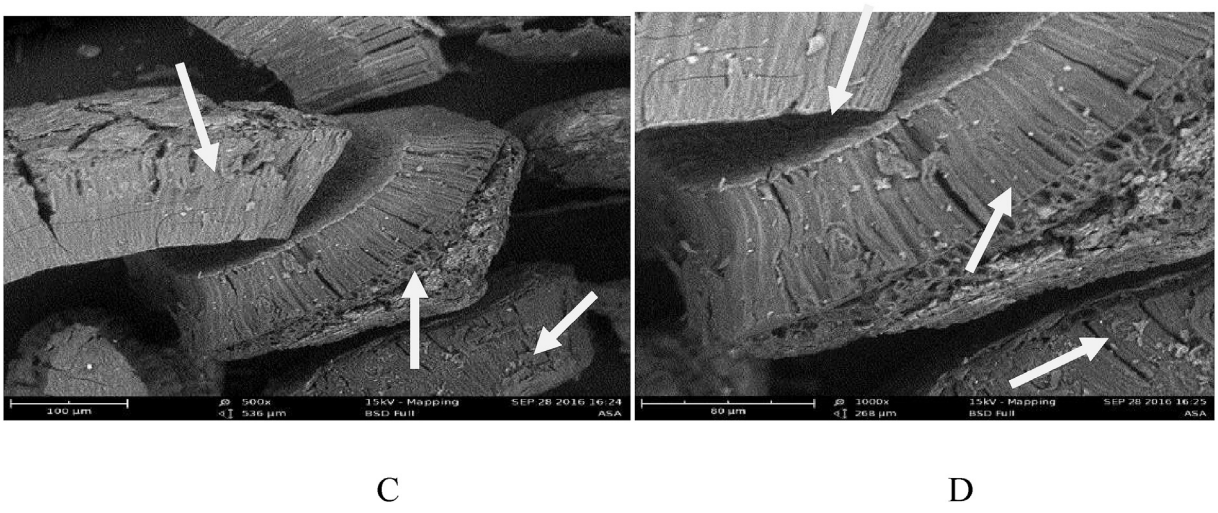

Fig. 5. SEM representations of almond shell after adsorption at different magnifications (C) 500, (D) 1000.

spectrophotometer, the existing heavy metals within the wastewater model were examined. The ASS analysis discovered the concentrations of total Cr, Cu (II), Mn (II), Co (II), and Pb (II) ions. The preliminary concentrations of the metal ions existing in the wastewater are shown in Table 1. From the outcomes, Cr and Cu (II) ions concentrations extremely exceeded the threshold limit and therefore, for the purpose of this study these would be the metals to be focused upon for their removal.

Table 1
Initial concentration of metal ions in tannery wastewater.

Metals	Initial Concentration (mg/L)
Total Cr	67.4660
Cu(II)	6.9766
Pb(II)	2.1584
Mn(II)	1.0435
Co(II)	0.0630
pH	3.7

3.3. Effect of process variables

3.3.1. Effect of flow rate

The column was operated at three varying flow rates of 3.0 ml/min, 6.0 ml/min and 9.0 ml/min at bed depth of 7.0 cm, almond shell powder of 16.1 g and initial metal concentration of 67.5 and 7.0 mg/L for Cr ions and Cu (II) ions respectively. The breakthrough curves obtained are illustrated in Fig. 6(A) for Cr ions and Fig. 6(B) for Cu (II) ions adsorption. Fig. 6 demonstrated that the breakthrough time and the bed exhaustion time reduces with the rise in flow rate from 3.0 to 9.0 ml/min for Cr ions and Cu (II) adsorption. This was due to rapid saturation of the bed because of increase in influent flow rate. This means that at greater flow rate, the rate of mass transfer rises and thus resulting into an increase in the quantity of metals Cr ions and Cu (II) ions adsorbed onto the unit bed height (mass transfer zone). The breakthrough curve formed steep gradient at higher flow rate for both metals adsorption. A greater flow rate led to a lesser residence time in the column and vice versa [43]. Also, increase in the flow rate reduces the interaction period between the metals ions (Cr and Cu (II) ions) and the almond shells. This result into a rise in the capacity of effluent treated.

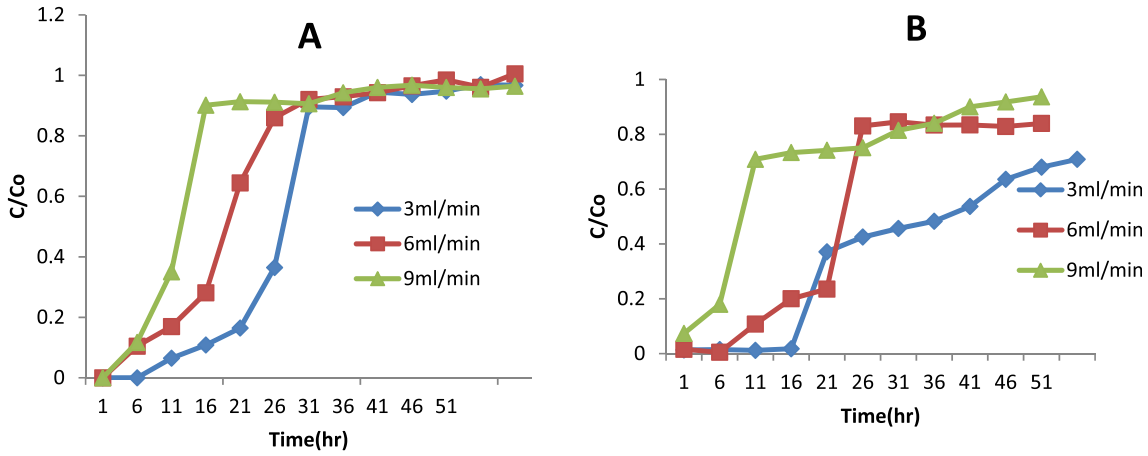

Fig. 6. Breakthrough curves for (A) Cr ions and (B) Cu(II) ions adsorption against almond shells at varying flow rates (bed depth = 7.0 cm, inlet Cr and Cu(II) concentrations of 67.5 mg/L and 7 mg/L respectively).

Table 2 shows the column data obtained from the experimental runs at varying flow rates. The column data result shows that as the flow rate increases from 3.0 to 9.0 ml/min, the volume of influent treated increases from 7920 ml to 23,760 ml and the percentage removal of Cr ions and Cu(II) decreases from 65.88 to 33.06% and 70.00 to 32.80% respectively. This revealed a higher proportion removal of the metal ions at low flow rate because the resident time increased thus, giving more way for metal ions to distribute into the pores of the almond shell via intra-particle diffusion. An increased flow rate signifies an inadequate time for metals ions to diffuse to the pores of the almond shell, resulting into decreased percentage removal.

3.3.2. *Effect of bed height*

The bed depth is an essential parameter for the design of a fixed bed column for continuous wastewater treatment plant. The breakthrough curves at different bed heights (3, 5 and 7 cm) of almond shell in the removal of Cr ions and Cu (II) from tannery wastewater at a flow rate of 3.0 ml/min and metals concentration of 67.5 mg/L and 7 mg/L for Cr ions and Cu (II) is presented in Fig. 7A and B respectively. The results demonstrate that the total volume of the aqueous solution rose with increase in bed height, owing to higher sorption sites as reported by Ref. [44]. The result in Table 3 indicates that increase in bed height result into the equilibrium sorption capacity decrease from 30.07 mg/g to 21.92 mg/g and 3.90 mg/g to 2.41 mg/g for Cr ions and Cu (II) respectively. However, at lesser bed height the effluent adsorbate concentration ratio rose higher compared to that at a higher bed height. This is what is responsible for a shorter bed saturation time for smaller bed heights. Smaller bed height signifies fewer quantity of adsorbent. As the bed height increased, the metals ions had additional time in interaction with almond shell particles, leading to a greater uptake of Cu (II) and Cr ions in the column as contained in Table 3. Therefore, when the bed height increases, the percentage removal of the metal ions also increases. The sharp increase in the slope of Cr ions as compared to Cu (II) is due to lower affinity to the almond shell. The breakthrough curves in Fig. 8 should be broadened as depicted by Cu (II) mass transfer zone. Also, the result in Table 3 shows that when the bed height rises from 3.0 to 7.0 cm, the cumulative metal ions sent to the column rose from 453.60 to 534.60 mg for Cr ions and from 45.36 to 55.44 mg for Cu (II) ion respectively. The amount of metal ion adsorbed at bed heights of 3 and 7 cm was 207.52 and 352.30 mg for Cr ions while, 26.91 and 38.61 mg for Cu (II) ion was adsorbed at 3 and 7 cm bed height respectively. The results in Table 3 also revealed that Cu (II) ion had the highest percentage removal at all bed heights but this reduces at bed heights of 5 cm before increasing again at 7 cm. This is because the differences in the bed heights are very low as such remarkably changes cannot be ascertained. It was observed that is advisable to use at least four times the internal diameter of the column to avoid clogging, channelling and overflowing. This can be verified in the study of [45] when evaluating on the impact of column diameter on biosorption of Cd (II) ions.

3.3.3. *Effect of initial metal ions concentration*

The effect of changing the inlet metal concentration from 55 to 67.5 mg/L and 3.5–7.0 mg/L for Cr ions and Cu (II) respectively was studied at a constant bed depth of 7 cm and feed flow rate of 3.0 ml/min. The breakthrough curves are illustrated in Fig. 8(A and B).

A careful observation of Fig. 8 shows that the almond shells were spent quicker at greater adsorbate inlet concentration of 67.5 and 7 mg/L for Cr ions and Cu (II) ions respectively. That is, preliminary breakthrough point was attained at high-level concentration. The breakpoint time was obtained after 16, 12 and 7 h for 54, 62 and 70 mg/L respectively before it exceeded the threshold value for drinking water. A reduction in inlet concentration resulted to a prolonged breakthrough curve, demonstrating that a high-level capacity of solution was treated. This is because low concentration gradient results into a lengthier transport owing to a reduction in diffusion coefficient or mass transfer coefficient [46]. The column data obtained in the course of the experimental run for varied concentrations are summarised in Table 4. From the Table, adsorption capacities increased from 18.19 to 21.92 mg/g and from 1.03 to 2.41 mg/g for Cr and Cu (II) respectively. The increase in adsorption capacity and removal efficiency at higher concentrations is as

Table 2
Column efficiency for Cr and Cu(II) ions adsorption against almond shell at bed height 7.0 cm, and initial concentration of 67.5 mg/L and 7.0 mg/L for Cr and Cu(II) respectively at different flow rates.

Metal	Q (ml/min)	t_{total} (min)	V_{eff} (ml)	M_{total}(mg)	q_{total} (mg)	Removal (%)	q_e (mg/g)
Cr	3.0	2640	7920	534.60	352.30	65.88	21.92
	6.0	2640	15,840	1069.20	458.40	42.87	28.47
	9.0	2640	23,760	1603.80	530.23	33.06	32.90
Cu(II)	3.0	2640	7920	55.44	38.61	70.00	2.39
	6.0	2640	15,840	110.56	55.72	50.40	3.446
	9.0	2640	23,760	165.84	54.45	32.80	3.38

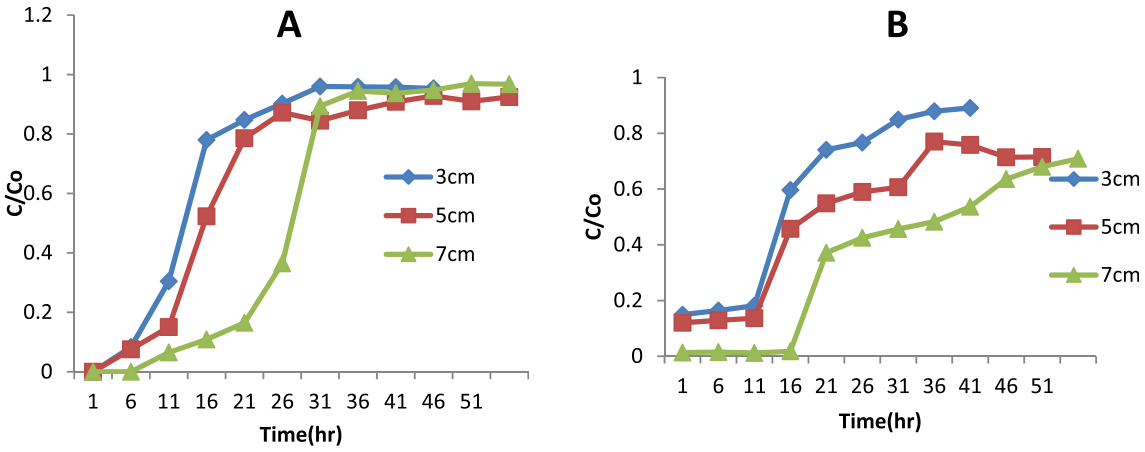

Fig. 7. Breakthrough curves for (A) Cr ions and (B) Cu(II) adsorption against almond shells at different bed depth (flow rates = 3.0 ml/min, inlet Cr ions and Cu(II) concentrations are 70 mg/L and 7 mg/L respectively).

Table 3
Sorption features for Cr and Cu (II) ions adsorption against almond shell at flow rate 3.0 ml/min, initial concentration of 70.0 mg/L and 7.0 mg/L for Cr (VI) and Cu (II) respectively for varying bed depth.

Metal	Z(cm)	t_{total} (min)	V_{eff} (ml)	M_{total}(mg)	q_{total} (mg)	Removal (%)	q_e (mg/g)
Cr(VI)	3.0	2160	6480	453.60	207.52	45.70	30.07
	5.0	2640	7920	534.60	270.43	50.50	23.52
	7.0	2640	7920	534.60	352.30	65.88	21.92
Cu(II)	3.0	2160	6480	45.36	26.91	59.30	3.90
	5.0	2640	7920	55.44	26.62	48.02	2.31
	7.0	2640	7920	55.44	38.61	70.00	2.41

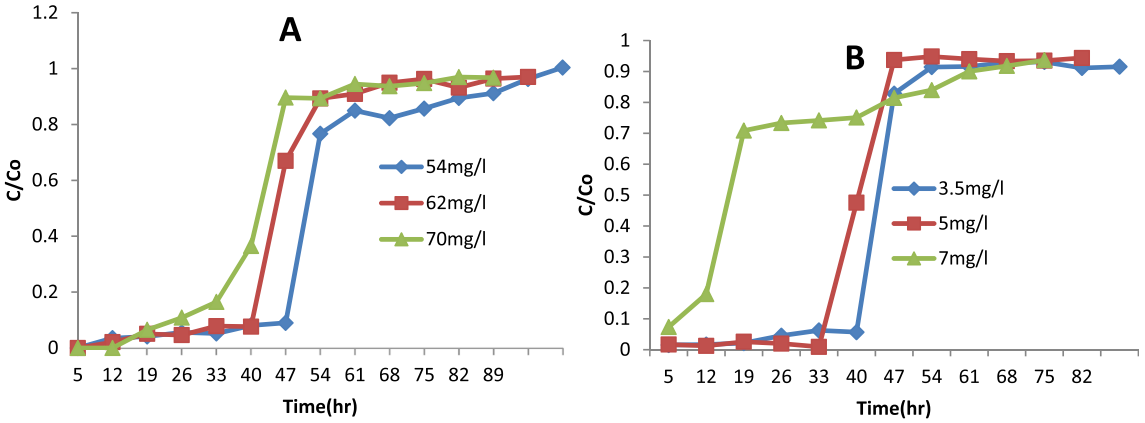

Fig. 8. Breakthrough curves for (A) Cr ions and (B) Cu (II) adsorption against almond shells at varied concentrations (flow rates = 3.0 ml/min, and bed depth = 7.0 cm).

Table 4
Sorption features for Cr ions and Cu (II) adsorption against almond shell at flow rate 3.0 ml/min, and bed depth of 7.0 cm for diverse inlet concentration.

Metal	C_0 (mg/L)	t_{total} (min)	V_{eff} (ml)	m_{total} (mg)	q_{total} (mg)	Removal (%)	q_e (mg/g)
Cr ions	55.0	3360	10,080	549.36	292.96	53.33	18.19
	60.0	3120	9360	579.38	289.71	50.00	17.99
	67.5	2640	7920	534.60	352.30	65.88	21.92
Cu (II)	3.5	3360	10,080	34.78	16.63	47.81	1.03
	5.0	3120	9360	46.89	20.69	44.12	1.28
	7.0	2640	7820	55.44	38.61	70.00	2.41

a result of the increase in solid and liquid phase, a driving force for the adsorption [45,46]which would help in scale-up or pilot plant when the column is operating at optimum conditions.

3.4. Kinetic modelling

3.4.1. Fitting of the thomas model

The effluent concentration-time profile (breakthrough curve)

Table 5
Thomas model parameters for Cr ions at different conditions.

Parameters	K_{TH}(ml/mg.min) x 10^{-2}	q_{calc} (mg/g)	q_{exp} (mg/g)	R_2
Flow rate (ml/min)				
3.0	4.43	17.79	21.92	0.991
6.0	4.37	23.06	28.47	0.963
9.0	2.77	26.01	32.90	0.811
Bed height (cm)				
3.0	3.23	27.46	30.07	0.920
5.0	3.70	21.17	23.52	0.948
7.0	4.44	17.79	21.92	0.991
Concentration (mg/L)				
55.0	4.63	18.47	18.91	0.953
60.0	5.85	16.14	17.99	0.967
67.5	4.44	17.79	21.92	0.991

Table 7
Yoon- Nelson model parameters for Cr ion sat various conditions.

Parameters	τexp (min)	τcalc (min)	Kyn x 10-4	R^2
Flow rate (ml/min)				
3.0	1320.00	1358.40	3.03	0.958
6.0	870.00	949.20	2.93	0.983
9.0	600.00	727.20	2.78	0.925
Bed height (cm)				
3.0	510.00	484.80	1.07	0.931
5.0	720.00	1079.40	2.32	0.921
7.0	1320	1358.40	3.03	0.958
Concentration (mg/L)				
55.0	1560.00	1834.20	2.50	0.963
60.0	1320.00	1365.00	3.70	0.955
67.5	1320.00	1358.40	3.03	0.958

obtained from the investigation was studied using Thomas model to establish how well the breakthrough data obtained correlated. The rate constant (K_{TH}) and maximum sorption capacity, q_0 (mg/g) were evaluated from the linear plots of ln(C_0/Ct-1) against time, t(min). The predicted values of K_{TH} and q_0 (mg/g) are listed in Tables 5 and 6 for chromium and copper respectively. The correlation coefficient R^2 obtained using this model ranges between 0.811 to 0.991 and 0.916 to 0.983 for Cr ions and Cu (II) ion respectively. The suitable fit of the experimental data with the Thomas model showed that the exterior and interior diffusion were not the limiting step [47]. The adsorption capacity (q_{calc}) calculated by the Thomas model in Tables 5 and 6 showed great agreement with those realised from the experimental results (q_{exp}). The results further revealed that for both metals, there was a decrease in rate constant (K_{TH}) when the effluent flow rate was increased from 3.0 ml/min to 9.0 ml/min. Also, K_{TH} rates rise with increase in bed height. The implication of this is that the breakthrough curve is positive at reduced flow rate and increased bed heights as reported by Ref. [40]. The adsorption capacities demonstrated a contrary trend, which increases with increase in flow rate. The decrease in K_{TH} as the concentration rises is as a result of the system being controlled by external mass transfer at the initial part of the column [46]. This is associated with increase in the adsorption capacity, q as previously reported by Ref. [47].

3.4.2. Application of Yoon and Nelson model

The experimental data of the almond shell adsorption of Cr ions and Cu (II) ion were fitted with Yoon-Nelson model to examine the breakthrough features of Cr ions and Cu (II) ions adsorption against the adsorbent. The rates of K_{YN} and τ were evaluated from the linear plots of (C_t/(C_o-C_t) versus t (min) at varying flow rates, bed heights, and preliminary metal ions concentration. The values of K_{yn} and τ for 50% breakthrough time (min) are presented in Tables 7 and 8 for chromium and copper respectively. The data were suitably fitted with Yoon-Nelson model with correlation coefficient, R^2 varying from 0.925 to 0.983 and 0.933 to 0.985 for chromium and copper respectively. The rate constant, K_{yn} increased with the increase in bed height and decreases with increase in flow rate for both Cr and Cu (II) ions. With increase in initial concentration, the values of K_{yn} decreases which could be an indication of the bed exhaustion and further removal of the metals ions is not feasible. The time needed for 50% exhaustion of column, τ (min) reduced with the increase in the flow rate and initial concentration but rose with increase in bed height. This agrees with the outcomes gotten by Ref. [44]. The drift towards the 50% column exhaustion duration was in accordance with the experimental data. The result in Tables 7 and 8 indicates that the breakthrough time for 50% breakthrough capacity of the column had great proximity with those predicted by the Yoon-Nelson model. The close values of correlation coefficients gotten in the two models demonstrate the adequacy of the two models used and a true reflection of the accuracy i. e data reported and predicted.

3.4.3. Application of modified dose response model

As illustrated on Tables 9 and 10, the dose response model showed good agreement with the correlation coefficient for Cu (II) ions effect using flowrate, bed heights and concentrations. This ranges from 0.7389 to 0.9398, while the adsorption capacity was 0.2959–2.5758. The reverse was the case for chromium ions. The correlations were lower but

Table 8
Yoon- Nelson model parameters for Cu (II) at various conditions.

Parameters	τ_{exp} (min)	τ_{calc} (min)	K_{yn} x 10^{-3}	R^2
Flow rate (ml/min)				
3.0	2040.00	2286.00	2.40	0.944
6.0	1320.00	1795.20	2.17	0.938
9.0	600.00	1238.95	1.90	0.933
Bed height (cm)				
3.0	900.00	1422.60	1.67	0.985
5.0	1080.00	1541.21	1.65	0.945
7.0	2040.00	2286.00	2.40	0.944
Concentration (mg/L)				
3.5	1560.00	1785.79	3.17	0.948
5.0	1500.00	1758.13	3.20	0.941
7.0	600.00	1238.95	1.90	0.933

Table 6
Thomas model parameters for Cu (II) at different conditions.

Parameters	K_{TH}(ml/mg.min)	q_{calc} (mg/g)	q_{exp} (mg/g)	R^2
Flow rate (ml/min)				
3.0	0.34	2.78	2.39	0.944
6.0	0.31	4.68	3.46	0.937
9.0	0.13	0.27	3.38	0.975
Bed height (cm)				
3.0	0.23	4.34	3.90	0.983
5.0	0.24	2.80	2.31	0.945
7.0	0.34	2.98	2.41	0.944
Concentration (mg/L)				
3.5	0.74	1.34	1.033	0.961
5.0	0.60	1.72	1.28	0.916
7.0	0.13	0.27	1.13	0.975

Table 9
Modified Dose Response Model parameters for Cr ion.

Parameters	a	b (ml)	q_{exp}	q_{cal}	R^2
Flow rate (ml/min)					
3.0	1.2008	1342.240	21.92	5.6246	0.3660
6.0	1.2219	2164.711	28.47	9.0712	0.4386
9.0	1.2809	1960.650	32.90	8.2161	0.6869
Bed height (cm)					
3.0	1.2398	904.690	30.07	3.7911	0.3077
5.0	1.1741	1521.000	23.52	6.3737	0.5063
7.0	1.0735	1456.000	21.92	6.1014	0.6527
Concentration (mg/L)					
55.0	1.1838	4027.000	18.91	13.7568	0.2976
60.0	1.5900	2529.300	17.99	9.4260	0.4038
67.5	1.0003	1539.570	21.92	6.4547	0.3249

Table 10
Modified Dose Response Model parameters for Cu(II).

Parameters	a	b (ml)	q_{exp}	q_{cal}	R^2
Flow rate (ml/min)					
3.0	1.6998	682.8102	2.39	0.2959	0.7389
6.0	2.0841	5973.103	3.46	2.5883	0.7926
9.0	1.3409	3916.52	3.38	1.6971	0.9397
Bed height (cm)					
3.0	1.0931	2122.76	3.90	0.9199	0.7769
5.0	0.9781	2939.680	2.31	1.2738	0.8283
7.0	1.6998	5944.29	2.41	2.5758	0.7389
Concentration (mg/L)					
3.5	2.2189	3598.32	1.033	0.7822	0.7011
5.0	2.5239	2941.03	1.28	0.9134	0.6270
7.0	1.3311	1317.95	1.13	0.5730	0.9398

with higher adsorption capacity in the range of 3.7911–13.7568. This could be as result of total chromium ions and not specifically the oxy-anions which are the Cr (VI) and Cr (III).

3.5. Error function analysis

Two models were verified in the analysis of the column data from experiment conducted in the removal of both copper and chromium metals from the ternary effluent. Based on the R^2 values (0.953–0.944) and the lower error functions (ERRSQ0.5808–0.2827, HYBRID 0.0812–1.9093 and MPSD 0.0016–0.0799) for Cr and Cu (II) ions respectively. Thomas model is observed to be the most suitably fitted model and therefore reliable since error function analysis approach has been referred to as the utmost efficient optimization tool to assess the best suitably fitted model for the column adsorption experimental data as reported by Ref. [48].

3.6. Comparison with other adsorbents

See Table 11.

3.7. Adsorption mechanism

The mechanism of Cr and Cu (II) ion uptake by the almond shell is proposed in the column adsorption process as shown in the graphical abstract. The almond shell has hydroxyl and phenol sets as the major functional groups participating in the reaction as indicated by the FTIR before and after adsorption. The material which contains several phenol and alcohol groups loses 2 protons per mol of the divalent cation at initial stage as demonstrated by the reaction scheme. In the subsequent stage, hydrated metallic ion loses its water of hydration. Meanwhile, in the third stage almond constituent uptakes the non-solvated metallic ion. At lesser pH value, the initial phase of the adsorption process is effective for sorption of Cr ions and ineffective for Cu (II) ions. However, at pH of 7, Cu (II) reaches its adsorption peak.

Table 11
Comparison of Cu (II) and Cr ions adsorption capacity of almond shell with other low-cost adsorbents.

Metal	Low-cost adsorbent	q (mg/g)	References
Copper (II)	*Kappaphycus* sp.	19.46	[49]
	Pine cone shell	6.52	[50]
	Acer saccharum leaves	18.30	[19]
	Calcium-alginate Shea Butter Cake	4.64	[51]
	Green coconut shell powder	285.70	[52]
	Raw Almond shell	2.41	This study
Chromium (VI)			
	Soy hull biomass	7.29	[39]
	Palm stems powder (PSP)	2.50	[53]
	PEI functionalised egg shell	160	[[52]
	Zizania caduciflora	2.70	
	Jatropha wood	140.8	
	Wheat bran modified using tartaric acid	5.28	[52]
	Pre-treated orange peel	7.6	
	Hydrochloric acid modified oak saw dust	1.7	
	Sulphuric acid modified pine sawdust	20.3	
	Egg shell	1.45	
	Egg shell modified using PEI	160	
	Eichhornia crassipes@dead biomass	5.6	[54]
	Raw Almond shell	21.92	This study

4. Conclusion

In the course of this analysis, the potentials of Cu (II) and Cr ions adsorption from real tannery effluent using almond shell in a continuous fixed bed column were investigated and evaluated. Findings from the research indicated that adsorption of these metal ions is highly influenced by influent metal concentration, bed height, and flowrate. The SEM characterization demonstrated that the almond shell has probable binding sites in its particles inner surface. Also, the FTIR showed that binding groups including carbonyl, hydroxyl, and phenols existed in the adsorbent. Adsorption of Cu (II) and Cr ions was more effective at higher adsorbate inlet concentration, high-level almond shell bed height, and lower feed flow rate. The cumulative amount of metals adsorbed, total percentage removal, and equilibrium metal uptake increased with increasing influent concentration. The optimum condition for the column was at flow rate of 3.0 ml/min, bed height of 7.0 cm, concentrations of 7.0 mg/L and 67.5 mg/L for Cu(II) and Cr ions correspondingly. The percentage removal of Cu (II) and Cr ions at optimum condition was found to be 70.0 and 65.9% with equivalent adsorption capacitiesof2.41 mg/g and 21.92 mg/g respectively. The investigative information obtained was corresponded with Thomas and Yoon-Nelson models. Substantial characteristics of the models like adsorption capacity (Thomas model) and duration for 50% breakthrough (Yoon- Nelson model) were established by linear regression analysis. All the kinetic models used in this work adequately represent the experimental breakthrough data obtained.

Declaration of competing interest

In this research work there are no conflicts of interest.

References

[1] Z. Liang, W. Shi, Z. Zhao, T. Sun, F. Cui, The retained templates as “helpers” for the spherical meso-silica in adsorption of heavy metals and impacts of solution chemistry, J. Colloid Interface Sci. 496 (2016) 382–390, https://doi.org/10.1016/j.jcis.2017.02.02410.1016/j.jcis.2017.02.024.
[2] M. Baláž, Z. Bujň-áková, P. Baláž, A. Zorkovská, Z. Danková, J. Briančin, Adsorption of cadmium (II) on waste biomaterial, J. Colloid Interface Sci. 454 (2015) 121–133, https://doi.org/10.1016/j.jcis.2015.03.04610.1016/j.jcis.2015.03.04610.22059/ijer.2011.320.
[3] S. Kang, J. Lee, K. Kima, Biosorption of Cr (III) and Cr ionsonto the cell surface of pseudomonas aeruginosa, Biochem. Eng. J. 36 (1) (2007) 54–58, https://doi.org/10.1016/j.bej.2006.06.00510.1016/j.bej.2006.06.005.
[4] S. Mehdipour, V. Vatanpour, H.-R. Kariminia, Influence of ion interaction on lead removal by a polyamide nanofiltration membrane, Desalination 362 (2015) 84–92, https://doi.org/10.1016/j.desal.2015.01.03010.1016/j.desal.2015.01.030.
[5] A. Tripathi, A.K. Dwivedi, Studies on recovery of chromium from tannery wastewater by reverse osmosis, J. Ind. Pollut. Contr. 28 (1) (2011) 29–34.
[6] K.K. Deepali, Gangwar, Metal concentration in textile and tannary effluents, Associated soils and ground water, New York science Journal 3 (4) (2010) 82–89.
[7] Z. Song, C.J. Williams, R.G.J. Edyvean, Treatment of tannery wastewater by chemical coagulation, Desalination 164 (3) (2004) 249–259, https://doi.org/10.1016/S0011-9164(04)00193-6.
[8] V. Sarin, K.K. Pant, Removal of chromium from industrial waste by using eucalyptus bark, Bioresour. Technol. 97 (1) (2006) 15–20, https://doi.org/10.1016/j.biortech.2005.02.01010.1016/j.biortech.2005.02.01010.1016/S0011-9164(04)00193-6.
[9] L. Rafati, A.H. Mahvi, A.R. Asgari, S.S. Hosseini, Removal of chromium (VI) from aqueous solutions using Lewatit FO_{36} nano ion exchange resin, Int. J. Environ. Sci. Technol. 7 (1) (2010) 147–156, https://doi.org/10.1007/BF0332612610.1007/BF0332612610.1007/BF03326126.

[10] N. Balan, Y. Otsuka, M. Nishioka, J.Y. Liu, G.J. Bailey, Physical mechanisms of the ionospheric storms at equatorial and higher latitudes during the recovery phase of geomagnetic storms, J. Geophys. Res. Space Physics 118 (5) (2013) 2660–2669, https://doi.org/10.1002/jgra.5027510.1002/jgra.50275.
[11] H.S. Gaber, M.A. El-Kasheif, S.A. Ibrahim, M.N. Authman, Effect of water pollution in el-rahawy drainage canal on hematology and organs of freshwater fish clariasgariepinus, World Appl. Sci. J. 21 (3) (2013) 329–341, https://doi.org/10.5829/idosi.wasj.2013.21.3.71192.
[12] S.R. Popuri, Y. Vijaya, V.M. Boddu, K. Abburi, Adsorptive removal of copper and nickel ions from water using chitosan coated PVC beads, Bioresour. Technol. 100 (1) (2009) 194–199, https://doi.org/10.1016/j.biortech.2008.05.04110.1016/j.biortech.2008.05.041.
[13] P. Xiangliang, W. Jianlong, Z. Daoyong, Biosorption of Pb(II) by Pleurotusostreatus immobilized in calcium alginate gel, Process Biochem. 40 (8) (2005) 2799–2803, https://doi.org/10.1016/j.procbio.2004.12.00710.1016/j.procbio.2004.12.007.
[14] M. Rhazi, J. Desbrieres, A. Tolaimate, M. Rinaudo, P. Vottero, A. Alagui, M. El Meray, Influence of the nature of the metal ions on the complexation with chitosan. Application to the treatment of liquid waste, Eur. Polym. J. 38 (8) (2002) 1523–1530, https://doi.org/10.1016/S0014-3057(02)00026-510.1016/S0014-3057(02)00026-5.
[15] M. Sharma, S. Hazra, S. Basu, Kinetic and isotherm studies on adsorption of toxic pollutants using porous ZnO and SiO_2 monolith, J. Colloid Interface Sci. 504 (2017) 669–679, https://doi.org/10.1016/j.jcis.2017.06.02010.1016/j.jcis.2017.06.020.
[16] I.E. Arshad, E.M. Minerva, A.H. Hisham, M.A. Farouk, Adsorption of heavy metals from industrial wastewater using palm date pits as low cost adsorbent, Int. J. Eng. Adv. Technol. 3 (5) (2014) 71–76.
[17] F. Fu, Q. Wang, Removal of heavy metal ions from wastewaters: a review, J. Environ. Manag. 92 (3) (2011) 407–418, https://doi.org/10.1016/j.jenvman.2010.11.01110.1016/j.jenvman.2010.11.011.
[18] A.A. Farghali, M. Bahgat, W.M.A. ElRouby, M.H. Khedr, Decoration of multi-walled carbon nanotubes (MWCNTs) with different ferrite nanoparticles and its use as an adsorbent, Journal of Nanostructure in Chemistry 3 (1) (2013) 50, https://doi.org/10.1186/2193-8865-3-5010.1186/2193-8865-3-5010.1186/2193-8865-3-50.
[19] S. Amirnia, M.B. Ray, A. Margaritis, Copper ion removal by Acer saccharum leaves in a regenerable continuous-flow column, Chem. Eng. J. 287 (2016) 755–764. https://dx.doi.org/10.1016/j.cej.2015.11.056.
[20] M. Imamoglu, O. Tekir, Removal of copper (II) and lead (II) ions from aqueous solutions by adsorption on activated carbon from a new precursor hazelnut husks, Desalination 228 (1–3) (2008) 108–113, https://doi.org/10.1016/j.desal.2007.08.01110.1016/j.desal.2007.08.011.
[21] G. Issabayeva, M.K. Aroua, N.M. Sulaiman, Study on palm shell activated carbon adsorption capacity to remove copper ions from aqueous solutions, Desalination 262 (1–3) (2010) 94–98, https://doi.org/10.1016/j.desal.2010.05.05110.1016/j.desal.2010.05.051.
[22] S. Idris, Y.A. Iyaka, B.E.N. Dauda, M.M. Ndamitso, M.T. Umar, Kinetic study of utilizing groundnut shell as an adsorbent in removing chromium and nickel from dye effluent, Am. Chem. Sci. J. 2 (1) (2012) 12–24, https://doi.org/10.9734/ACSJ/2012/90810.9734/ACSJ/2012/908.
[23] D. Sivakumar, Hexavalent chromium removal in a tannery industry wastewater using rice husk silica, Global Journal of Environmental and Science Management 1 (1) (2014) 27–40, https://doi.org/10.7508/gjesm.2015.01.00310.7508/gjesm.2015.01.003.
[24] S.V. Ashtikar, A.D. Parkhi, Adsorption of copper from aqueous solution using mango seed powder, Int. J. Eng. Res. Afr. 4 (4) (2014) 75–77.
[25] G.H. Pino, L.M. Souza de Mesquita, M.L. Torem, G.A.S. Pinto, Biosorption of cadmium by green coconut shell powder, Miner. Eng. 19 (5) (2006) 380–387, https://doi.org/10.1016/j.mineng.2005.12.00310.1016/j.mineng.2005.12.003.
[26] M. Nameni, M.R.A. Moghadam, M. Arami, Adsorption of hexavalent chromium from aqueous solutions by wheat bran, Int. J. Environ. Sci. Technol. 5 (2) (2008) 161–168, https://doi.org/10.1007/BF0332600910.1007/BF03326009.
[27] J. Anwar, U. Shafique, Waheed-uz-Zaman, M. Salman, A. Dar, S. Anwar, Removal of Pb(II) and Cd(II) from water by adsorption on peels of banana, Bioresour. Technol. 101 (6) (2010) 1752–1755, https://doi.org/10.1016/j.biortech.2009.10.02110.1016/j.biortech.2009.10.02110.1016/j.biortech.2009.10.021.
[28] M.D. Yahya, J.O. Odugure, I.A. Mohammed-Dabo, I.A. Mohammed, Utilization of Modified Shea Butter Husk as an Adsorbent for the Removal of Heavy Metals in Industrial Effluents, Academia-Industry (ACICON), 2014.
[29] H.J. Michael, L.V. Jose, Kinetic study of liquid-phase adsorptive removal of heavy Metal ions by almond tree (*terminalia catappa l.*) Leaves waste, Bull. Chem. Soc. Ethiop. 21 (3) (2007) 349–362, https://doi.org/10.4314/bcse.v21i3.2121610.4314/bcse.v21i3.21216.
[30] M. Kilic, E. Apaydin-Varol, E.A. Putun, Adsorptive removal of phenol from aqueous solutions on activated carbon prepared from tobacco residues: equilibrium, kinetics and thermodynamics, J. Hazard Mater. 189 (1–2) (2011) 397–403, https://doi.org/10.1016/j.jhazmat.2011.02.05110.1016/j.jhazmat.2011.02.051.
[31] M.A. Renu, K. Singh, Heavy metal removal from wastewater using various adsorbents: a review, Journal of Water Reuse and Desalination 7 (4) (2016) 387–419. https://doi:10.2166/wrd.2016.104.
[32] A. Raouf -Ms, A. Raheim-Arm, Removal of heavy metals from industrial wastewater by biomass-based materials: a review, Journal of Pollution Effects & Control 5 (1) (2017) 180, https://doi.org/10.4172/2375-4397.1000180.
[33] A.S. Ayangbenro, O.B. Olubukola, A new strategy for heavy metal polluted environments: a review of microbial biosorbents, Int. J. Environ. Res. Publ. Health 14 (1) (2017) 94, https://doi.org/10.3390/ijerph1401009410.3390/ijerph14010094.
[34] D.K. Singh, V. Kumar, S. Mohan, D. Bano, S.H.(Hassan, Breakthrough curve modeling of graphene oxide aerogel packed fixed bed column for the removal of Cr(VI) from water, Journal of Water Process Engineering (18) (2017) 150–158, https://doi.org/10.1016/j.jwpe.2017.06.01110.3390/ijerph14010094.
[35] M.D. Yahya, J.O. Odigure, Fixed bed column study for Pb(II) adsorption using calsium alginate shea butter husk. 2015 International conference on industrial Engineering and operations management (IEOM) held at Dubai, United Arab Emirates on 3-5 March 2015. https://doi.org/10.1109/IEOM.2015.7093936https://doi.org/10.1109/IEOM.2015.7093936, 2015.
[36] C.M. Futalan, C.C. Kan, M.L. Dalida, C. Pascua, M.W. Wan, Fixed-bed column studies on the removal of copper using chitosan immobilized on bentonite, Carbohydr. Polym. 83 (2) (2011) 697–704, https://doi.org/10.1016/j.carbpol.2010.08.04310.1016/j.carbpol.2010.08.043.
[37] M.A. Martin-Lara, G. Blazquez, A. Ronda, I.L. Rodriguez, M. Calero, Multiple biosorption-desorption cycles in a fixed-bed column for Pb(II) removal by acid treated olive stone, J. Ind. Eng. Chem. 18 (3) (2012) 1006–1012, https://doi.org/10.1016/j.jiec.2011.11.15010.1016/j.jiec.2011.11.150.
[38] Z.Z. Chowdhury, S.M. Zain, A.K. Rashid, R.F. Rafique, K. Khalid, Breakthrough curve analysis for column dynamics sorption of Mn(II) ions from wastewater by using mangostana garcinia peel-based granular-activated carbon, Journal of Chemistry, 2013 (2013) 1–8, https://doi.org/10.1155/2013/959761.
[39] P.S. Blanes, M.E. Bordoni, J.C. González, S.I. García, A.M. Atria, L.F. Sala, S.E. Bellú, Application of soy hull biomass in removal of Cr ionsfrom contaminated waters. Kinetic, thermodynamic and continuous sorption studies, Journal of Environmental Chemical Engineering 4 (1) (2016) 516–526, https://doi.org/10.1016/j.jece.2015.12.00810.1016/j.jece.2015.12.00810.1016/j.jece.2015.12.008.
[40] Z. Aksu, F. Gönen, Biosorption of phenol by immobilized activated sludge in a continuous packed bed: prediction of breakthrough curves, Process Biochem. 39 (5) (2004) 599–613, https://doi.org/10.1016/S0032-9592(03)00132-8.
[41] N. Ozturk, D. Kavak, Adsorption of boron from aqueous solutions using fly ash: batch and column studies, J. Hazard Mater. 127 (1–3) (2005) 81–88, https://doi.org/10.1016/j.jhazmat.2005.06.026.
[42] I. Khazaei, M. Aliabadi, H.T.(Hamed-Mosavian, Use of agricultural waste for removal of Cr ionsfrom aqueous solution, Iranian Journal of Chemical Engineering 8 (4) (2011) 11–23.
[43] M.A. Acheampong, K. Pakshirajan, A.P. Annachhatre, P.N.L. Lens, Removal of Cu (II) by biosorption onto coconut shell in fixed-bed column systems, J. Ind. Eng. Chem. 19 (3) (2013) 841–848, https://doi.org/10.1016/j.jiec.2012.10.029.
[44] J.T. Nwabanne, P.K. Igbokwe, Adsorption performance of packed bed column for the removal of lead (ii) using oil palm fibre, Int. J. Appl. Sci. Technol. 2 (5) (2012) 106.
[45] M.F. Ahmad, S. Haydar, Evaluation of a newly developed biosorbent using packed bed column for possible application in the treatment of industrial effluents for removal of cadmium ions, Journal of the Taiwan Institute of Chemical Engineers 62 (2016) 122–131, https://doi.org/10.1016/j.jtice.2015.12.03210.1016/j.jtice.2015.12.032.
[46] A.A. Ahmad, B.H. Hameed, Fixed-bed adsorption of reactive azo dye onto granular activated carbon prepared from waste, J. Hazard Mater. 175 (1–3) (2010) 298–303, https://doi.org/10.1016/j.jhazmat.2009.10.003.
[47] A. Ghribi, M. Chlendi, Modelling of fixed bed adsorption: application to the adsorption of an organic dye, Asian J. Textil. 1 (4) (2011) 161–171, https://doi.org/10.3923/ajt.2011.161.171.
[48] S. Biswas, U. Mishra, Continuous fixed-bed column study and adsorption modeling: removal of lead ion from aqueous solution by charcoal originated from chemical carbonization of rubber wood sawdust, Journal of Chemistry, 2015 (2015) 1–9, https://doi.org/10.1155/2015/90737910.1155/2015/907379.
[49] M.D. Sayedur- Rahman, V.(Kathiresan-Sathasivam, Heavy metal adsorption onto kappaphycus sp. from aqueous solutions: the use of error functions for validation of isotherm and kinetics models, BioMed Research International, 2015 (2015) 1–13, https://doi.org/10.1155/2015/12629810.1155/2015/126298.
[50] M.A. Martín-Lara, G. Blázquez, M. Calero, A.I. Almendros, A. Ronda, Binary biosorption of copper and lead onto pine cone shell in batch reactors and in fixed bed columns, Int. J. Miner. Process. 148 (2016) 72–82, https://doi.org/10.1016/j.minpro.2016.01.01710.1016/j.minpro.2016.01.017.
[51] M.D. Yahya, I.A. Mohammed-Dabo, A.S. Ahmed, A.S. Olawale, Copper (II) adsorption by calcium-alginate shea butter cake, Civ. Environ. Res. 3 (4) (2013) 20–38.
[52] M.A. Renu, K. Singh, Heavy metal removal from wastewater using various adsorbents: a review, Journal of Water Reuse and Desalination 7 (4) (2017) 387–419, https://doi.org/10.2166/wrd.2016.10410.2166/wrd.2016.104.
[53] S. Nouacer, S. Hazourli, R. Djellabi, F.Z. Khelaifia, R. Hachani, M. Ziati, Using a new lignocellulosic material based on palm stems for hexavalent chromium adsorption in aqueous solution, Int. J. Environ. Res. 10 (1) (2016) 41–50, https://doi.org/10.22059/ijer.2016.5688610.22059/ijer.2016.56886.
[54] S. Saraswat, J.P.N. Rai, Heavy metal adsorption from aqueous solution using Eichhorniacrassipes dead biomass, Int. J. Miner. Process. 94 (3–4) (2010) 203–206, https://doi.org/10.1016/j.minpro.2010.02.00610.1016/j.minpro.2010.02.006.